Published by SET Publisher

Journal of Basic & Applied Sciences

ISSN (online): 1927-5129

Magnetized Seeds and Structured Water: Effects on Resilience of Velvet Bean Seedlings (*Mucuna pruriens*) under Deficit Irrigation

Craig L. Ramsey*

Retired – USDA, Fort Collins, CO, 80526, USA

Article Info:

Keywords:
Structured Water,
Deficit Irrigation,
Vapor Pressure Deficit,
Biotic Resilience,
Macroscopic Coherence,
Quantum Biology,
Whole Plant Water Use Efficiency.

Timeline:
Received: November 15, 2023
Accepted: December 08, 2023
Published: December 31, 2023

Citation: Ramsey CL. Magnetized seeds and structured water: Effects on resilience of velvet bean seedlings (*Mucuna pruriens*) under deficit irrigation. J Basic Appl Sci 2023; 19: 249-270.

DOI: https://doi.org/10.29169/1927-5129.2023.19.19

Abstract:

A custom-built water generator supplied structured water (SW) for applying the deficit irrigation treatments to velvet bean plants (*Mucuns pruriens*). The objectives of the study were to 1) determine the effects of magnetized seed treatment on velvet bean plants, 2) determine the effects of magnetized and hydroxylated water treatments on velvet bean plants, and 4) determine the effects of deficit irrigation, using three soil moisture levels, on velvet bean plants. The optimal water-saving treatment was magnetized seeds plus 10 MT + HWT. This treatment had a 226% increase in transpiration and a 22% increase in water vapor concentration in the intercellular airspace for the low soil moisture watering schedule. The three study factors in the optimal seed and water treatment had a synchronistic effect for enhancing metabolic efficiency by increasing whole plant WUE by 87% and carbon assimilation efficiency by 66% in the low soil moisture schedule. Plants irrigated with SW water and grown from magnetized seeds had enhanced resilience to high water stress conditions by maintaining adequate levels of biologically structured water. The rapid deactivation of a suite of highly interconnected defense activities in the optimal seed and water treatments implies that the plants exhibit macroscopic coherence properties. Coherence at the macroscopic level resulted in complex synchronization between metabolic efficiency, plant health, and deactivation of a suite of regulatory defenses in plants exposed to high water stress.

*Corresponding Author
E-mail: clramsey37@gmail.com

1. INTRODUCTION

This article reports on a more detailed gas exchange analysis of a study previously published by Ramsey [1]. In the two years since the first article was published, further analyses of unexplored gas exchange variables revealed significant findings explaining why structured water (SW) increased biotic resilience and drought tolerance in velvet bean seedlings (*Mucuna pruriens*). These expanded findings focus on water vapor dynamics, leaf, and gas exchange variable interactions with the study factors. A hypothesis of this study was that irrigating plants with SW water should maintain biologically structured water (BSW) at normal water tissue levels, even for plants grown under high water stress conditions. These latest results indicate that water-stressed plants with adequate or normal levels of BSW water maintained macroscopic coherence so that plants could simultaneously optimize metabolic efficiency and minimize plant injury.

Structured water has an expanded hydrogen-bonded water network with stronger hydrogen bonds (H-bonds), resulting in supramolecular or polymeric clusters of water molecules mixed with free water with weaker H-bonds [2 – 5]. Most natural water sources comprise about 20 - 40% SW water at room temperature. The SW:Free water structure ratio can be increased dramatically using several methods to strengthen the H-bonds in free water. SW water properties include higher viscosity, lower vapor pressure, and increased electrical conductivity and pH [6 - 12]. Electrical conductivity increases in SW water due to the supramolecular clusters of hexamer water rings with delocalized and quasi-free electrons and protons in the π orbitals above and below each cyclic water ring [13 - 18]. When unstructured, liquid water is exposed to chemical and electromagnetic energy sources that cross the ionization threshold of water, a percentage of the water molecules will ionize and split into hydronium ions ($H3O^+$) and hydroxyl radicals (•OH) [19 - 21]. These ions and radicals will then reform back into SW water.

This study investigated the effects of SW irrigation water on water stressed plants. As the SW water is taken up by the plant roots and transported into the foliage, it is converted into Biologically Structured Water (BSW). The functions, roles, and properties of BSW water are suited to sustain life and are different from SW water. BSW water is synonymous with other research terms such as tightly bound, exclusion zone (EZ), vicinal water, interfacial, hexagonal, non-freezing, or liquid crystalline water. A full description of splitting liquid water into hydroxyl radicals to generate SW water is published in Part 3 of the review of BSW water.

A custom-built hydroxylated water system was designed for this study using a combination of three energy sources to generate SW water for the plant irrigation treatments. The closed-loop water system included a water pump, hose lines, a hydroxyl generator, static magnets, a 132 L water tank, and a control panel (Image **1**). The hydroxyl generator component utilized ultraviolet lamps to convert water vapor in the air into ozone. The ozonated water was then converted into hydroxyl free radicals and hydronium ions (H_3O^+) [19 - 21]. The hydroxyl free radicals and hydronium ions partially reform back to water molecules with stronger H-bonds that form SW water with hexamer water rings [22 - 24]. Static neodymium magnets were also placed next to the water tube in the water generator to increase the structured water ratio in the irrigation water. The closed-loop system allowed the water to recirculate and pass through the hydroxyl generator numerous times. As the exposure time increased, water structure also increased.

Image 1: Photo of custom-built water generator that generated this study's water treatments.

This second article from the original study [1] focuses on the effects of the three study factors on leaf water content dynamics for plants under high water stress. It also tested the effects of magnetized seeds and SW water on regulatory plant responses to water stress, increased efficiencies, and enhanced resilience to abiotic stress. Gas exchange data was collected 34 to 37 days after starting the second deficit irrigation schedule. The gas exchange data was analyzed for the low soil moisture treatments that lasted about 35 - 40 days after starting the initial deficit irrigation schedule. The following water content variables were analyzed: leaf vapor pressure deficit (vpdl), saturated vapor pressure in the leaf (SVTleaf), saturated vapor pressure in air (SVTair), water vapor concentration inside the leaf (h2o_l), difference in water vapor concentration between inside leaf and the air (h2o_diff), air temperature (tair), and leaf temperature (Tleaf). Saturated vapor pressure is computed from vapor pressure and temperature, and water vapor concentration is computed from SVP and atmospheric pressure.

The spongy mesophyll inside of leaves contains intercellular airspaces near the stomatal openings. These airspaces allow the phase transition of BSW water into water vapor, which is an endothermic process that cools the foliage [25 – 28]. As transpiration increases, the phase transition rate increases with increased cooling due to the endothermic dynamics of water converting to water vapor. These airspaces also allow CO_2 to enter the plant and diffuse into the chlorophyll sites to initiate photosynthesis. The intercellular airspace volume is estimated to be about 70% of the leaf volume [29]. The intercellular airspaces contain water vapor and CO_2, and these variables can be measured in units of pressure (kPa) or units of mole fractions (mol H_2O or CO_2/ mol air). Until recently, it was widely assumed that the airspaces within the spongy mesophyll were saturated with water vapor and had a saturated vapor pressure near 99% [25]. This assumption has been challenged by researchers who suggest that leaf airspaces are undersaturated [26, 28]. Whether the intercellular airspace is saturated or unsaturated with water vapor has important implications for estimating the leaf vapor pressure deficit (vpdl) in leaves [27]. The leaf vapor pressure can be estimated from air temperatures if the airspace in the leaf is assumed to be saturated. The gas exchange program in the LICOR 6400 instrument assumes that vapor pressure in the intercellular airspaces is fully saturated. Therefore, SVTleaf was computed from a leaf temperature model.

The interrelationships between vapor pressure dynamics within leaves, leaf temperature, and atmospheric conditions are complex and highly interconnected [28 - 31]. Water vapor pressure is the pressure (kPa) exerted by water in the gas phase in a closed system. Water vapor pressure inside the leaf determines the rate at which water transitions from liquid to vapor. The higher the vapor pressure at a given temperature, the weaker the H-bonds in the liquid water, and evaporation rates increase [26, 28]. Saturated Vapor Pressure (kPa) is the pressure at which water vapor is in thermodynamic equilibrium with its liquid phase. Leaf Vapor Pressure Deficit (kPa) is the difference in the air's Saturated Vapor Pressure (SVP) and Relative Humidity outside of the leaf, i.e., vpdl is the difference between SVTair and RHair.

Another set of analyses tested the effects of SW water on several plant efficiency indices. These efficiency parameters included Whole-plant water use efficiency (WUE), leaf cooling efficiency, and carbon assimilation efficiency. Whole plant WUE is the integrated water use parameter that divides plant biomass accumulated over the course of the study by the accumulated water volume used over the study. This study estimated the whole plant WUE from the accumulated, aboveground, oven-dried plant biomass divided by the average daily watering volume for each seed and water treatment for each soil moisture target (g biomass/ml daily water). The leaf cooling efficiency is estimated by dividing leaf temperature by air temperature (Tleaf/Tair). Finally, the carbon assimilation index was estimated by dividing the average daily biomass growth rate by the rate of photosynthesis (g biomass/day)/Pn (umol $CO_2/m^2/s$)). A comparison of these efficiency indices between the control and optimal seed and water treatment will test whether the optimal treatment enhanced overall plant efficiency or not.

The plant species selected for this drought tolerance study was the velvet bean (*Mucuna pruriens*). This tropical legume has a C3 Calvin cycle pathway that exhibits photoinhibition defense responses to protect against free radical damage in chlorophyll when plants are water-stressed. Velvet bean is a fast-growing, twining vine with limited drought tolerance that is often used as a cover crop [32]. Due to its rapid growth rates and large leaf area, the plants have high foliage gas exchange rates, making it an ideal species for this study.

2. MATERIALS AND METHODS

The greenhouse study was conducted in Fort Collins, CO. Greenhouse parameters were set at ambient light conditions, and a temperature range was set at 26 to 35 C. The study design involved a factorial model with the four study factors fully crossed with each other to test the main effects and all interactions among the study factors. The study factors included three soil moisture levels, two seed treatments, three magnet treatments, and two hydroxylated water generator treatments.

2.1. Seed Treatments

Velvet bean (*Mucuna pruriens*) seeds included two seed treatments, which were non-magnetized (NMS) and magnetized (MS) seeds. The control treatment seeds were soaked in water for three hours before planting without exposure to any magnetic fields. The magnetized seeds were soaked in water while placed on a static magnet for three hours before planting. A neodymium static magnet (grade N-42) was used with the South Pole face of the magnet facing up into the seeds. After soaking, the seeds were coated with a powder form of *Rhizobium leguminosarum* (N-Dure, INTX Microbials, Kentland, IN) before planting. The rhizobium species is specific for legumes and is a gram-negative bacteria used to inoculate legume roots to start nitrogen-fixing colonies in root nodules. Each pot was planted with eight coated seeds. All germinated seeds were culled down to the two most vigorous seedlings at the two-cotyledon leaf stage. Two velvet bean plants were grown in each pot until the completion of the study.

2.2. Pot and Soil Description

The wood fiber pots had a soil volume of 4.87 l and a water saucer volume of 800 ml (Western Pulp Products Co. Corvallis, OR). Sixty-four (64) pots were filled with potting soil, which was a mix of Canadian sphagnum peat moss, processed pine bark, vermiculite, and perlite mix (Farfard – 4-MP, Sun Gro Horticulture, Agawam, MA). A controlled release fertilizer (19-5-6 NPK) (FloriKote CRF, Florikan ESA, Sarasota, FL) was applied at ten g/pot 11 days after planting (DAP).

2.3. Magnetic Water Treatments

This study used two grades (grades N-42 and N-52) of static neodymium magnets (K&J Magnets, Inc., Pipersville, PA). The large cylinder magnets (N-42) were 7.6 cm diam x 5.1 cm thick, and the small cylinder magnets (N-52) were 5.1 cm diam x 2.5 cm thick. There are three magnetic field treatments: 1) control, or no magnets on hydroxyl water generator or water hoses (0-MT), 2) two N-42 neodymium magnets placed on the top cover of hydroxyl water generator (2-MT, and 3) two N-42 neodymium magnets placed on the top cover of hydroxyl water generator, and 10 N-52 neodymium magnets placed on the water hose between generator and water tank (10-MT). The ten N-52 magnets were placed on top of a steel U-shaped channel beam with the water hose inserted into the U channel. The magnetized water treatments were combined with or without the hydroxylated water treatments, depending on the assigned water treatment run for that day.

All neodymium magnets had their South Pole facing the water hose or the hydroxyl water generator. The measured strength at the magnet surface was 493 and 510 mT for the N-42 and N-52 neodymium magnets, respectively. However, both magnets were placed at different distances from the water hoses or the hydroxylated water column. The measured strength of the N-42 magnet at 7.6 cm from the water column in the hydroxyl generator was 45 mT. The measured strength of the N-52 magnet at 5 cm from the water hoses was 131 mT. The static magnets were removed or replaced daily, depending on the water treatment assigned to be generated on that day.

2.4. Hydroxylated Water Treatments and Closed Loop System Description

The hydroxylated water generator was a commercial unit for recreational water treatment for swimming pools (EcoMaster PZ-784, Prozone Water Products, Huntsville, AL). The generator was slightly modified by placing static magnets on the metal surface of the generator, just above the quartz water line running through the generator. The hydroxyl generator operates by allowing air to enter the unit, where two hybrid UVC lamps (287 nm wavelength) convert the air and water vapor into ozone (O_3) and hydroxyls ($OH^{\cdot}$). Water enters the generator through a venturi injector drawing O_3 and $OH^{\cdot}$ from the lamp chamber. A static mixer combines water, O_3, and OH into a micro-bubble water flow. The ozonated water passes through a quartz water column radiated with the two UVC lamps, which converts the ozonated water into hydroxyl radicals. The two hydroxylated water treatments were: 1) hydroxyl water generator turned on (HWT), or 2) hydroxyl water generator turned off (NHWT).

The hydroxylated water generator was a component of the closed-loop water system that was custom-built by Spartan Environmental Technologies [19]. The closed loop system was run for 30 min. to generate each batch for a specific water treatment. This study had six water treatments (3 MT x 2 HWT = 6 WT), and one water treatment was generated per day due to the time required for each run. Each water treatment was stored in a labeled 19 l container for three days before making a new batch. In other words, each water treatment batch was stored after it was generated and then used to irrigate the assigned pots over three days before generating a new water treatment batch. The water treatments were generated on a rotating basis. Each water treatment could be run with or without the hydroxylated water generator turned on or the static magnetics placed on the water hoses or the generator. The water pump capacity was 3.78 l/min. The water tank and total water hose capacity was 118 l. The water turnover rate for a full water tank was 10.9 times for each 30 min. water treatment run, i.e., for each water treatment, the water was exposed to a combination of magnetics and hydroxylated water generator 10.9 times before collecting and storing the treated water. The control water (0 MT + NHWT) was run in the closed loop system for 30 min. without the hydroxylated water generator being turned on or the magnets placed on the water hoses. All water lines and the tank were purged between each water treatment run.

2.5. Soil Moisture Levels and Soil Moisture Methods

Deficit irrigation was conducted by hand watering to achieve three soil moisture levels ranging from intense water stress to fully saturated soil moisture. The three soil moisture levels were based on volumetric soil moisture (SM) levels, which were:

1) low soil moisture (LSM) (10 to 15% v/v)

2) moderate soil moisture (MSM) (15 to 20% v/v SM)

3) high soil moisture (HSM) (20 to 25% soil moisture).

The soil moisture level targets were implemented after the seedlings reached the second set of trifoliate leaves approximately 21 days after planting.

All pots were well watered with tap water between seed planting and the second trifoliate stage so that the seedlings were well established with long roots before starting the deficit irrigation treatments. All pots were randomly assigned to the three soil moisture levels and water treatments. The first set of soil moisture levels were too high, and the plants showed no wilting symptoms. At 21 days after planting, daily watering was reduced, and soil moisture was monitored until the three soil moisture target levels were reached.

Daily volumetric soil moisture measurements were collected using a data logger and a soil moisture and temperature sensor (ECH2O EM-50 data logger and 5-TM soil sensor, METER Environmental, Pullman, WA). Each pot was measured every morning between 8 and 10 am using a single datalogger and a 5-TM soil probe, and the data was hand-recorded. The sensors were buried so that soil moisture readings were collected at approximately 5 – 10 cm.

2.6. Daily Soil Moisture Measurements and Watering Methods

Volumetric soil moisture (SM) readings were collected with a data logger and soil moisture sensors (ECH2O data logger and 5-TM soil sensors, METER Environmental, Pullman, WA). METER scientists developed an equation to adjust the default algorithm based on mineral soil. Potting soil is virtually organic, and the raw tensiometer data was converted to percent soil moisture data using an algorithm suited for organic soil. The daily soil moisture measurements were hand-recorded and used to estimate the daily water volume needed to maintain each pot at its label or assigned irrigation target. Each pot's water volume was adjusted daily based on its growth rate and irrigation target.

All 64 pots were watered daily after estimating the water volume to apply to each pot. Treated water stored in the 19 l containers was added to smaller pails to fill a 500- or 1,000-ml volumetric cylinder to record precise water volumes per pot. The daily water volume was compiled into a single dataset for study factor analyses or as a covariate in the study analyses.

2.7. Foliage Gas Exchange Methods

A LICOR 6400 XT gas exchange instrument (LICOR Environmental, Lincoln, NE) was used to measure leaf and atmospheric variables. Gas exchange data was collected 58 – 64 days after planting and 37 days after starting the three deficit irrigation treatments by hand watering each pot. The foliage measurements included: photosynthesis (Pn),

stomatal conductance (g), transpiration (E), RH-air = relative humidity in leaf sample, SVTleaf = saturated vapor pressure in leaf, SVTair = saturated vapor pressure in air, h2o_l = water vapor concentration inside leaf., leaf vapor pressure deficit (vpdl), and leaf temperature (ltemp). Vapor pressure deficit is a driver for transpiration due to the difference between the actual vapor pressure and the saturation vapor pressure at a set temperature. Direct measurements of leaf water contents are difficult to quantify, and indirect measurements involve computations with assumptions built into the model parameters. The assumptions in the LICOR 6400 SVTleaf model in this study are based on tap water properties and not on SW water properties. This discrepancy in tap and SW water properties will be discussed in more detail in the Discussion section of this article.

The LICOR 6400 parameters are set as: Leaf ratio = 0.5, PAR = 800 umol/m^2/s, block temperature = 35 C, and flow rate = 400, and CO_2 = 400 mg/l. The uppermost, fully mature leaves were selected for gas exchange measurements. Three leaves per plant were selected: dark green or mature leaves with no disease spots inside the measurement area. All gas exchange measurements include six replicates (2 plants x 3 leaves = six replicates per treatment) without including any hidden replication that is described in the Data Analyses section. Soil moisture data was collected along with the gas exchange parameters, and all the parameters were combined into a single dataset so that soil moisture could be tested as a covariate in the data analyses.

2.8. Data Analyses

The study design included hidden replication for the statistical modeling analysis. Hidden replication restricts the interaction tests to only two-way interactions. The SAS JMP (SAS Institute Inc., Clary, NC) Design of Experiment (DOE) generated 16 replications of the whole plots for biomass and water volume data analyses. The DOE design for whole plot replication included hidden replicates by limiting the analysis to only two-way interactions without considering three or four-way interactions. The sample size for the gas exchange data was 41, which also included hidden replication by limiting the analysis to two-way interactions.

Multivariate analysis was conducted to test for correlations among the gas exchange leaf and air variables. Pairwise comparisons among these variables generated detailed, individualized tables with correlation strength and *p*-values for each pair of variables. The SAS JMP Restricted Maximum Likelihood (REML) model analyzed the foliar gas exchange data. This model included variation among the three leaves as a random variable. The JMP Least Squares Fit (LSF) model was used to test treatment effects for average percent soil moisture, cumulative water volume, oven-dry foliage biomass, and plant water use efficiency. Analysis results were deemed to be significant if *p*-values were less than 0.05. Error bars in graphs represent the standard error of model values.

The pairwise correlation test included five tables for a selected set of seed and water treatments for the low soil moisture study factor. The five correlation tables include 1) Control, 2) Optimal Treatment, 3) Revised Optimal Treatment #1, 4) Revised Optimal Treatment #2, and 5) Revised Optimal Treatment #3. The optimal treatment was magnetized seed plus 10-MT + HWT. In other words, the optional treatment had magnetized seeds, all ten magnets attached to the water line, and the hydroxylated water generator was turned on. The revised optimal treatments tested the effects of changing one study factor at a time for the optimal treatment. For example, for the revised optimal treatment #1, only the hydroxylated water treatment was turned off, while the other two factors remained unchanged. This pairwise correlation tested the effects of the hydroxyl generator compared to the correlation table with all three factors turned on. The optimal #2 tested non-magnetized seeds while keeping the other two study variables the same. Optimal #3 treatment tested the effects of neodymium magnets on the water lines while keeping the other two study factors the same.

3. RESULTS

The velvet bean plants were allowed to twine up bamboo stakes over the 64-day study. Photos were taken during the last week of the study, just before the plants were harvested, and they showed that the plants were healthy and still vigorously growing (Images **2-4**).

The average percent soil moisture was graphed to show the daily temporal dynamics and general range patterns for the three target soil moisture levels from 13 to 52 days after the initiation of the study (Figure **1**). The average soil moisture from 13 to 52 days was 12, 18, and 23% for the LSM, MSM, and HSM soil moisture levels. Due to the daily monitoring and water schedule,

Image 2. Photo of velvet bean plants at 60 DAP for the control treatment (0-MT + NHWT).

Image 3. Photo of velvet bean plants (center of photo) at 60 DAP for the two magnets + hydroxylated water treatment (2-MT + HWT).

Image 4. Photo of velvet bean plants (center of photo) at 60 DAP for the ten magnets + hydroxylated water treatment (10-MT + HWT).

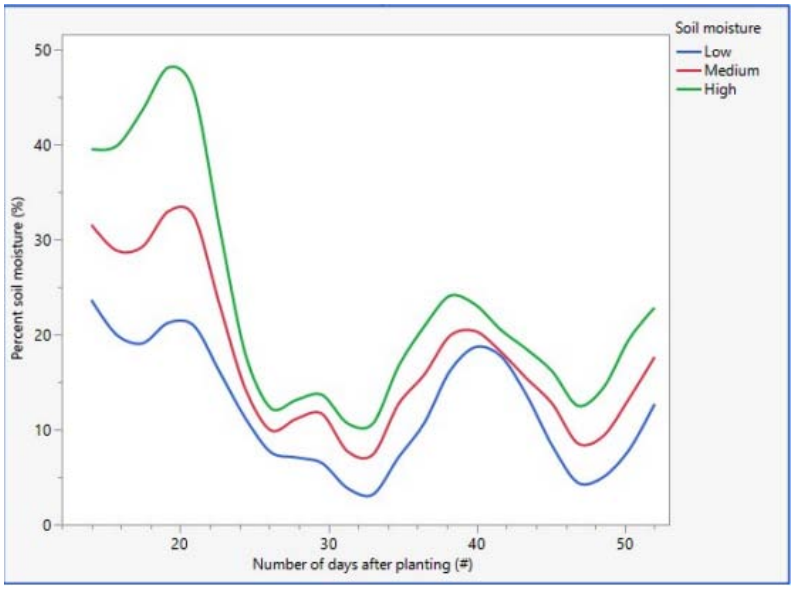

Figure 1: Average daily percent soil moisture was measured between 13 and 52 days of the study. A statistical smoother curve plotted soil moisture over time for the three soil moisture levels (legend) and was averaged across the magnetized seed and water treatments. Soil moisture was reduced to the adjusted soil moisture levels after the 21st day.

the three target soil moisture levels were kept within a narrow range when averaged across magnetized seed and structured water treatments. The drop in soil moisture from 17 to 24 days after planting was due to readjusting soil moisture levels to induce higher water stress levels in the plants. The higher water stress levels ensured that the magnetized seed and structured water treatments were tested on truly water-stressed plants that simulated drought conditions.

The Least Squared Fit model tested the effects of the magnetized seed and structured water treatments on the percent soil moisture (Table **1**). The model included all four study factors and three two-way interaction terms. The three other study factors reported Average percent soil moisture for magnetized and non-magnetized seed treatments (Tables **2**, **3**). The magnetized seed combined with the 18 structured water treatments shows that the percent soil moisture was higher in the 2-MT + HWT and 10-MT + HWT treatments than in the associated magnetized seed treatments with 0-MT + NHWT water treatment under the LSM soil moisture level (Table **2**). The non-magnetized seed treatments resulted in an even larger increase in percent soil moisture for the 2-MT + HWT and 10-MT + HWT treatments than in the associated magnetized seed treatments with 0-MT + NHWT water treatment under the LSM soil moisture level (Table **3**). For both seed treatments, the structured water treatments (2-MT + HWT and 10-MT + HWT) increased the LSM soil moisture levels due to lower transpiration rates (Figure **1**).

Table 1: Description of the Least Square Fit Model Terms and *p*-Values for Soil Moisture (m^3/m^3) Averaged 13 and 52 Days after Planting

Source	Prob > F
Magnetized seed	0.2155
Magnetized water	0.0009*
Hydroxyl Generator	0.9677
Soil moisture level	<.0001*
Mag seed* Soil moisture level	<.0001*
Mag water* Soil moisture level	<.0001*
Hydroxyl generator* Soil moisture level	0.0004*

Analysis of the cumulative water volume per pot for each treatment shows that only the magnetized water factor and the soil moisture level were terms in the final model (Table **4**). The two other study factors (seed and HWT factors) were not in the final model due to the small sample size for each treatment. However, since the cumulative water volume per plant is such an important measurement in this study, the total water volumes were reported for all four study factors to fully understand the effects of the factors on water usage (Table **5**). Based on the cumulative water volumes, the optimal water-saving treatments were either magnetized or non-magnetized seed treatment combined with the 10-MT + HWT structured water treatment (Table **5**). The relative change for total water volume used represents the water use savings in the

Table 2: Based on Volumetric Data (m3/m3), the Average Percent Soil Moisture for the Magnetized Seed Treatment, by Structured Water Treatment, Hydroxyl Generator Status, and Soil Moisture Level. Soil Moisture was Averaged between 13 to 52 Days after Planting

Structured water trt	Hydroxyl generator	Soil moisture Level (%)	Percent soil moisture (%)	Relative change
0-MT + NHWT	No	10 -15	5	0
0-MT + NHWT	No	15 – 20	14	0
0-MT + NHWT	No	20 - 25	16	0
0-MT + HWT	Yes	10 -15	7	0
0-MT + HWT	Yes	15 – 20	12	0
0-MT + HWT	Yes	20 - 25	16	0
2-MT + NHWT	No	10 -15	10	100
2-MT + NHWT	No	15 – 20	14	0
2-MT + NHWT	No	20 - 25	21	31
2-MT + HWT	Yes	10 -15	14	100
2-MT + HWT	Yes	15 – 20	10	-17
2-MT + HWT	Yes	20 - 25	23	44
10-MT + NHWT	No	10 -15	16	220
10-MT + NHWT	No	15 – 20	14	0
10-MT + NHWT	No	20 - 25	14	-13
10-MT + HWT	Yes	10 -15	19	171
10-MT + HWT	Yes	15 – 20	10	-17
10-MT + HWT	Yes	20 - 25	16	0

[a]Relative change = (0-MT + NHWT – 2 or 10-MT + NHWT)/ 0-MT + NHWT) x 100) for each associated hydroxyl generator and soil moisture level.

Table 3: Average Volumetric Soil Moisture (m^3/m^3) for Non-Magnetized Seed Treatment by Structured Water Treatment, Hydroxyl Generator Status, and Soil Moisture Level. Soil Moisture was Averaged between 13 to 52 Days after Planting

Structured water trt	Hydroxyl generator	Soil moisture Level (%)	Percent soil moisture (%)	Relative change
0-MT + NHWT	No	10 -15	2	0
0-MT + NHWT	No	15 – 20	21	0
0-MT + NHWT	No	20 - 25	16	0
0-MT + HWT	Yes	10 -15	5	0
0-MT + HWT	Yes	15 – 20	16	0
0-MT + HWT	Yes	20 - 25	19	0
2-MT + NHWT	No	10 -15	7	250
2-MT + NHWT	No	15 – 20	19	-10
2-MT + NHWT	No	20 - 25	21	31
2-MT + HWT	Yes	10 -15	10	100
2-MT + HWT	Yes	15 – 20	14	-13
2-MT + HWT	Yes	20 - 25	23	21
10-MT + NHWT	No	10 -15	14	600
10-MT + NHWT	No	15 – 20	19	-10
10-MT + NHWT	No	20 - 25	14	-13
10-MT + HWT	Yes	10 -15	16	220
10-MT + HWT	Yes	15 – 20	16	0
10-MT + HWT	Yes	20 - 25	16	-16

[a]Relative change = (0-MT + NHWT – 2 or 10-MT + NHWT)/ 0-MT + NHWT) x 100) for each associated hydroxyl generator and soil moisture level.

Table 4: Description of the Least Squares Fit Model Terms and *p*-Values for the Cumulative Water Volume Added Per Plant. Daily Water Volumes Per Plant were Summed between 27 and 52 Days after Planting to Determine the Cumulative Water Volume

Source	Prob > F
Magnetized water	0.0001*
Soil moisture level	<.0001*
Magnetized*Soil moisture level	<.0001*

last two columns in Table **5**. Depending on the three soil moisture levels, the water use savings ranged from 29% to 49% for the 10-MT +HWT structured water treatment. The cumulative water volume for the 10- MT +HWT water structure is in general agreement with the percent soil moisture findings, i.e., the 10-MT + HWT treatment increased the percent soil moisture compared to the 0-MT + NHWT water treatment (Tables **2**, **3**). The structured water treatments used more water than the 0-MT + NHWT treatment in three out of six water treatments (Table **5**).

The pairwise correlations included gas exchange, leaf, and air status variables for only the low soil moisture study factor. An explanation for the pairwise correlation tables was given in the data analysis section above. The five correlation tables allow a detailed examination of the interplay between eight gas exchange, leaf, and air variables (Tables **6-10**). Overall, the correlation tables show complex interactions among leaf, water vapor, foliage water, and atmospheric conditions reflected in the gas exchange responses, leaf, and atmospheric parameters.

The pairwise table for the control treatment (Table **6**) shows significant correlations among the variables for the control treatment (non-magnetized seed and 0-MT + NHWT treatment). The correlations between gas exchange variables and leaf and atmospheric conditions mirrored the expected plant responses to high water stress conditions. Stomatal conductance, transpiration, and photosynthesis are all highly correlated. Also, stomatal conductance and transpiration negatively correlated with leaf and air temperature and leaf and air saturated vapor pressure.

Table 5: Cumulative Total Water Volume Per Plant Reported for Magnetized Water Treatment, Hydroxyl Treatment, and Three Soil Moisture Levels. The Total Water Volume was Reported for Daily Watering between 13 to 52 Days of the Study

Water trt	Hydroxyl Generator	Soil moisture level (%)	The sum for Mag seed water volume added (ml) per plant	The sum for Non-Mag seed water volume added (ml) per plant	Water savings for magnet seeds	Water savings for non-magnet seeds
0-MT	No	10 -15	20000	20950	0.0	0.0
0-MT	No	15 – 20	11800	11250	0.0	0.0
0-MT	No	20 - 25	15600	14950	0.0	0.0
0-MT	Yes	10 -15	18150	20150	0.0	0.0
0-MT	Yes	15 – 20	24450	22600	0.0	0.0
0-MT	Yes	20 - 25	30550	30400	0.0	0.0
2-MT	No	10 -15	14500	15450	-27.5	-26.3
2-MT	No	15 – 20	23450	19550	98.7	73.8
2-MT	No	20 - 25	25850	26700	65.7	78.6
2-MT	Yes	10 -15	13300	14600	-26.7	-27.5
2-MT	Yes	15 – 20	22100	21900	-9.6	-3.1
2-MT	Yes	20 - 25	23900	23700	-21.8	-22.0
10-MT	No	10 -15	19450	16700	-2.8	-20.3
10-MT	No	15 – 20	20100	20650	70.3	83.6
10-MT	No	20 - 25	19950	21450	27.9	43.5
10-MT	Yes	10 -15	10650	8900	-41.3	-55.8
10-MT	Yes	15 – 20	19650	18350	-19.6	-18.8
10-MT	Yes	20 - 25	10600	12500	-65.3	-58.9

[a]Water saving is based on relative change between water and control treatments. Relative change = (0-MT - 2 or 10-MT)/ 0-MT) x 100) for each associated hydroxyl generator, magnetized seed treatment, and soil moisture level.

Table **6** has 24 significant correlations among all the pairwise comparisons. Also, there are eight negative and ten positive correlations among the variables. Six correlations with extreme *p*-values (0.999 to 1.0) indicated that matching variables were used in both correlation pairs to estimate the variables. The pairwise correlations with near-perfect *p*-values should be ignored.

A casual observation of the significant correlations in Table **6** shows high interconnectivity among the gas exchange variables. The tables only included eight variables due to the lack of space in each table. Another six soil and atmospheric variables were also included in a pairwise correlation test. All six of these gas exchange variables also had significant correlations for the low soil moisture target for the control treatment (data not shown). The interconnectivity of as many as 14 variables indicates the complex physiological balance in plants exposed to water stress conditions. The tables estimate the correlation strength between each pair of variables.

In contrast to the control treatment, the optimal treatment (Table **7**) reveals only one significant *p*-value among all the pairwise correlations for the correlation between stomatal conductance and transpiration. The other three correlations use the same underlying parameter terms in the variable calculations; therefore, the correlations reach unity (1.0) and are thus irrelevant. The optional treatment included magnetized seeds, ten magnets attached to the water line, and the hydroxylated water generator switched on. This combination of seed and water treatments almost eliminated all significant correlations among the eight variables.

Water-stressed plants have a reduction in many gas exchange responses. The first article details the gas exchange responses for all the seed and water treatments [1]. The decrease in gas exchange responses for the control treatment confirms the expected reduction in these responses for plants grown under the low soil moisture treatment. However, the optimal seed and water treatment had several unexpected responses.

As the introduction mentions, saturated vapor pressure (SVTleaf) is a fundamental water variable that regulates the overall water dynamics of plants under water stress. As expected, SVTleaf was negatively correlated with stomatal conductance and transpiration. In contrast, there was no correlation between these gas exchange responses and SVTleaf for the optimal seed and water treatment. The control and optimal SVTleaf values were 5.15 and 5.23 kPa, respectively, for the low soil moisture treatments. The saturated vapor pressure (SVTleaf) for the optimal seed and water treatment was significantly higher than the control. The JMP REML test shows that the control and optimal SVTair values were 5.30 and 5.37 kPa for the low soil moisture treatments and were equivalent. The effect of SVTleaf on water dynamics in the leaves will be examined in more detail in the discussion section.

Table 6: Multivariate Test for Only Low SM Target (10 – 15%). A Pairwise Correlation Table for the Control Treatment Included Non-Magnetized Seeds and 0-MT + NHWT Water Treatment. Correlations are Negative or Positive, and Significant Correlation Probabilities are in Red Text

Pairwise Correlations

Variable	by Variable	Correlation	Signif Prob
Trmmol	Cond	0.9867	0.0003*
Tair	Cond	-0.6859	0.1325
Tair	Trmmol	-0.6981	0.1230
Tleaf	Cond	-0.8493	0.0324*
Tleaf	Trmmol	-0.8522	0.0312*
Tleaf	Tair	0.9640	0.0019*
RH_S	Cond	-0.5832	0.2244
RH_S	Trmmol	-0.6670	0.1478
RH_S	Tair	0.8747	0.0225*
RH_S	Tleaf	0.8344	0.0389*
SVTleaf	Cond	-0.8500	0.0320*
SVTleaf	Trmmol	-0.8542	0.0303*
SVTleaf	Tair	0.9629	0.0020*
SVTleaf	Tleaf	0.9999	<.0001*
SVTleaf	RH_S	0.8360	0.0381*
SVTair	Cond	-0.8197	0.0458*
SVTair	Trmmol	-0.8254	0.0431*
SVTair	Tair	0.9772	0.0008*
SVTair	Tleaf	0.9984	<.0001*
SVTair	RH_S	0.8495	0.0323*
SVTair	SVTleaf	0.9982	<.0001*
h2o_l	Cond	-0.8491	0.0325*
h2o_l	Trmmol	-0.8540	0.0304*
h2o_l	Tair	0.9634	0.0020*
h2o_l	Tleaf	0.9999	<.0001*
h2o_l	RH_S	0.8386	0.0370*
h2o_l	SVTleaf	1.0000	<.0001*
h2o_l	SVTair	0.9983	<.0001*

[a]Photo = photosynthesis, Trmmol = transpiration, Cond = stomatal conductance, tair = air temperature, tleaf = leaf temperature, RH-S = relative humidity in leaf sample, SVTleaf = saturated vapor pressure in leaf, SVTair = saturated vapor pressure in air, h2o_l = water vapor concentration inside leaf.

Table 7: Multivariate Test for Only Low SM Target (10 – 15%). A Pairwise Correlation Table for the Optimal Treatment Included Magnetized Seeds and 10-MT + HWT Water Treatment. Correlations are Negative or Positive, and Significant Correlation Probabilities are in Red Text.

Pairwise Correlations

Variable	by Variable	Correlation	Signif Prob
Trmmol	Cond	0.9985	0.0352*
Tair	Cond	0.8562	0.3456
Tair	Trmmol	0.8263	0.3809
Tleaf	Cond	0.1915	0.8773
Tleaf	Trmmol	0.1370	0.9125
Tleaf	Tair	0.6711	0.5317
RH_S	Cond	0.6363	0.5609
RH_S	Trmmol	0.5927	0.5962
RH_S	Tair	0.9434	0.2153
RH_S	Tleaf	0.8790	0.3164
SVTleaf	Cond	0.1918	0.8771
SVTleaf	Trmmol	0.1372	0.9124
SVTleaf	Tair	0.6713	0.5315
SVTleaf	Tleaf	1.0000	0.0002*
SVTleaf	RH_S	0.8792	0.3162
SVTair	Cond	0.4217	0.7228
SVTair	Trmmol	0.3710	0.7581
SVTair	Tair	0.8295	0.3772
SVTair	Tleaf	0.9707	0.1545
SVTair	RH_S	0.9678	0.1619
SVTair	SVTleaf	0.9708	0.1543
h2o_l	Cond	0.1882	0.8795
h2o_l	Trmmol	0.1336	0.9147
h2o_l	Tair	0.6685	0.5338
h2o_l	Tleaf	1.0000	0.0022*
h2o_l	RH_S	0.8774	0.3185
h2o_l	SVTleaf	1.0000	0.0023*
h2o_l	SVTair	0.9699	0.1566

[a]Photo = photosynthesis, Trmmol = transpiration, Cond = stomatal conductance, tair = air temperature, tleaf = leaf temperature, RH-S = relative humidity in leaf sample, SVTleaf = saturated vapor pressure in leaf, SVTair = saturated vapor pressure in air, h2o_l = water vapor concentration inside leaf.

Another water vapor variable (H2O_diff) measures the difference in relative water vapor concentration (mmol H_2O/mol air) between the leaf airspaces (H2O_l) and air (H2O_a). These water vapor variables, H2O_diff and SVTleaf, measure two different vapor conditions (concentration and pressure) within the leaves [55]. The H2O_diff for the control and optimal seed and water treatment was 27.47 and 45.72 mmol H_2O/mol air, respectively. Also, the H2O_l for the control and optimal seed and water treatment was 88.32 and 107.78 mmol H_2O/mol air, respectively. In other words, the optimal seed and water treatment

Table 8: Multivariate Test for Only Low SM Target (10 – 15%). A Pairwise Correlation Table for a Study Treatment Included Magnetized Seeds and 10-MT + NHWT Water Treatment but Excluded the Hydroxylated Generator. Correlations are Negative or Positive, and Significant Correlation Probabilities are in Red Text

Pairwise Correlations

Variable	by Variable	Correlation	Signif Prob
Trmmol	Cond	0.8293	0.0412*
Tair	Cond	-0.2963	0.5686
Tair	Trmmol	-0.7560	0.0821
Tleaf	Cond	-0.3682	0.4726
Tleaf	Trmmol	-0.6593	0.1544
Tleaf	Tair	0.8544	0.0303*
RH_S	Cond	-0.2674	0.6085
RH_S	Trmmol	-0.7334	0.0972
RH_S	Tair	0.9991	<.0001*
RH_S	Tleaf	0.8605	0.0278*
SVTleaf	Cond	-0.3618	0.4810
SVTleaf	Trmmol	-0.6477	0.1643
SVTleaf	Tair	0.8474	0.0332*
SVTleaf	Tleaf	0.9997	<.0001*
SVTleaf	RH_S	0.8541	0.0304*
SVTair	Cond	-0.3556	0.4891
SVTair	Trmmol	-0.7000	0.1215
SVTair	Tair	0.9177	0.0099*
SVTair	Tleaf	0.9904	0.0001*
SVTair	RH_S	0.9224	0.0088*
SVTair	SVTleaf	0.9886	0.0002*
h2o_l	Cond	-0.3622	0.4804
h2o_l	Trmmol	-0.6449	0.1668
h2o_l	Tair	0.8432	0.0350*
h2o_l	Tleaf	0.9996	<.0001*
h2o_l	RH_S	0.8500	0.0321*
h2o_l	SVTleaf	1.0000	<.0001*
h2o_l	SVTair	0.9874	0.0002*

[a]Photo = photosynthesis, Trmmol = transpiration, Cond = stomatal conductance, tair = air temperature, tleaf = leaf temperature, RH-S = relative humidity in leaf sample, SVTleaf = saturated vapor pressure in leaf, SVTair = saturated vapor pressure in air, h2o_l = water vapor concentration inside leaf.

(magnetized seed plus 10 MT + HWT) had 19.46 mmol H_2O/mol air more water vapor in the intercellular airspaces than the control treatment. The increase in water vapor pressure (SVTleaf) and concentration (H2O_l) in the leaves of the optimal treatment suggests that even small increases in SVTleaf or H2O_l may alter or shut down a full suite of plant defense activities associated with water-stressed plants.

Table 9: Multivariate Test for Only Low SM Target (10 – 15%). A Pairwise Correlation Table for a Study Treatment Included Non-Magnetized Seeds and 10-MT + HWT Water Treatment that Excluded the Magnetized Seed Treatment. Correlations are Negative or Positive, and Significant Probabilities are in Red Text

Pairwise Correlations

Variable	by Variable	Correlation	Signif Prob
Trmmol	Cond	0.9995	0.0208*
Tair	Cond	-0.0636	0.9595
Tair	Trmmol	-0.0310	0.9803
Tleaf	Cond	-0.5333	0.6419
Tleaf	Trmmol	-0.5054	0.6627
Tleaf	Tair	0.8781	0.3176
RH_S	Cond	0.2812	0.8186
RH_S	Trmmol	0.3123	0.7978
RH_S	Tair	0.9399	0.2219
RH_S	Tleaf	0.6619	0.5395
SVTleaf	Cond	-0.5341	0.6413
SVTleaf	Trmmol	-0.5063	0.6620
SVTleaf	Tair	0.8776	0.3182
SVTleaf	Tleaf	1.0000	0.0006*
SVTleaf	RH_S	0.6611	0.5402
SVTair	Cond	-0.4401	0.7099
SVTair	Trmmol	-0.4105	0.7307
SVTair	Tair	0.9241	0.2496
SVTair	Tleaf	0.9943	0.0680
SVTair	RH_S	0.7380	0.4715
SVTair	SVTleaf	0.9942	0.0686
h2o_l	Cond	-0.5274	0.6464
h2o_l	Trmmol	-0.4994	0.6671
h2o_l	Tair	0.8814	0.3132
h2o_l	Tleaf	1.0000	0.0045*
h2o_l	RH_S	0.6671	0.5351
h2o_l	SVTleaf	1.0000	0.0051*
h2o_l	SVTair	0.9950	0.0636

[a]Photo = photosynthesis, Trmmol = transpiration, Cond = stomatal conductance, tair = air temperature, tleaf = leaf temperature, RH-S = relative humidity in leaf sample, SVTleaf = saturated vapor pressure in leaf, SVTair = saturated vapor pressure in air, h2o_l = water vapor concentration inside leaf.

The three sets of pairwise correlations in Tables **8-10** were designed to answer how each of the three study factors affected the gas exchange responses if they were not included in the optimal seed and water treatment. Table **8** tested the effects of the hydroxylated water generator when it was turned off in the optimal treatment. Table **9** tested the effects of non-magnetized seeds in the optimal treatment. Table **10**

Table 10: Multivariate Test for Only Low SM Target (10 – 15%). A Pairwise Correlation Table for a Study Treatment Included Magnetized Seeds and 0-MT + HWT Water Treatment but Excluded the Neodymium Magnet Treatment. Correlations are Negative or Positive, and Significant Probabilities are in Red Text

Pairwise Correlations

Variable	by Variable	Correlation	Signif Prob
Trmmol	Cond	0.9526	0.0033*
Tair	Cond	0.0583	0.9126
Tair	Trmmol	-0.0857	0.8718
Tleaf	Cond	-0.8098	0.0508
Tleaf	Trmmol	-0.5958	0.2120
Tleaf	Tair	-0.4019	0.4296
RH_S	Cond	0.7831	0.0655
RH_S	Trmmol	0.8945	0.0161*
RH_S	Tair	-0.5091	0.3024
RH_S	Tleaf	-0.3121	0.5470
SVTleaf	Cond	-0.8027	0.0545
SVTleaf	Trmmol	-0.5865	0.2211
SVTleaf	Tair	-0.4121	0.4169
SVTleaf	Tleaf	0.9999	<.0001*
SVTleaf	RH_S	-0.2995	0.5641
SVTair	Cond	-0.8342	0.0390*
SVTair	Trmmol	-0.6273	0.1824
SVTair	Tair	-0.3028	0.5596
SVTair	Tleaf	0.9944	<.0001*
SVTair	RH_S	-0.3812	0.4559
SVTair	SVTleaf	0.9931	<.0001*
h2o_l	Cond	-0.8036	0.0541
h2o_l	Trmmol	-0.5878	0.2198
h2o_l	Tair	-0.4134	0.4152
h2o_l	Tleaf	0.9999	<.0001*
h2o_l	RH_S	-0.3001	0.5633
h2o_l	SVTleaf	1.0000	<.0001*
h2o_l	SVTair	0.9930	<.0001*

[a]Photo = photosynthesis, Trmmol = transpiration, Cond = stomatal conductance, tair = air temperature, tleaf = leaf temperature, RH-S = relative humidity in leaf sample, SVTleaf = saturated vapor pressure in leaf, SVTair = saturated vapor pressure in air, h2o_l = water vapor concentration inside leaf.

tested the effects of not including the neodymium magnets in the optimal treatment. The correlation results show that as each study factor was not included in the optimal treatment, the pairwise correlations changed. Also, the study factors synergistically improved the gas exchange results when all three factors were included in the optimal treatment.

The pairwise correlations in Table **8** show that the hydroxylated water generator significantly impacted the correlation results. In contrast, excluding the magnetized seeds had little impact on the correlation results (Table **9**). When the neodymium magnets were excluded from the optimal treatment, three pairwise correlations were significant and not computed using the same basic temperature parameters. These results show a synergistic effect on the gas exchange responses by combining all three study factors into the optimal seed and water treatment.

Gas exchange estimates were predicted using the JMP REML models for the low and high soil moisture target treatments (Table **11**). These predicted values will differ slightly from the gas exchange estimates reported in the first article [1]. The difference between the soil and gas exchange predictions in the first article and Table **11** in this article is due to how the REML models included soil moisture in the Profiler predictions. In the REML models used in Table **11** in this article, the average soil moisture for the specific treatment was entered into the Profiler model, which predicted slightly different results than reported in the first article [1].

The model results in Table **11** allow comparisons between the control and optimal seed and water treatments. Stomatal conductance, transpiration, SVTleaf, H2O_l, and soil moisture increased for the optimal seed and water treatment. Transpiration for the optimal treatment increased by 226 and 143%, respectively, for the low and high soil moisture treatment, respectively, compared to the control treatment. The predicted gas exchange values for the

Table 11: Gas Exchange Estimates Based on the JMP REML Model for the Control (Non-Magnetized Seed Plus 0-MT +NHWT) and Optimal (Magnetized Seed Plus 10-MT +HWT) Treatment. The Gas Exchange, Leaf, and Water Usage Estimates are Listed for the Low and High Soil Moisture Treatments

Variable	Control at Low soil moisture	Control at High soil moisture	Optimal at Low soil moisture	Optimal at High soil moisture
Photosynthesis (umol $CO_2/m^2/s$)	10.41	9.35	5.92	5.9
Transpiration (mol $H_2O/m^2/s$)	0.89	1.35	2.9 *	3.28
Stomatal Cond. ($mol/m^2/s$)	0.01	0.06	0.07	0.08
Vpdl (kPa)	1.7	0.09	2.99 *	3.09
Leaf temp. (C)	35.3	33.2	35.0	35.7
Ci/Ca	1.4	1.0	0.44	0.39
SVTleaf (kPa)	5.07	5.6	5.14 *	6.1
H2O_l (mmol H_2O/mol air)	88.54	84.8	107.63 *	106.93
Soil moisture ((% v/v)	2	16	19	16
Sum of water volume added (ml)	20,950	14,950	10,650	10,600
Average Daily Watering volume (ml)	403	288	205	204
Total above-ground, oven-dry biomass (g/plant)	32.9	43.7	31.1	42.0
Whole plant water use efficiency (total biomass g/ave. daily ml/plant)	0.08	0.15	0.15	0.21

[a]vpdl = vapor pressure deficit for leaf, Ci/Ca = ratio of internal CO_2 to atmosphere CO_2, SVTleaf = saturated vapor pressure in leaf, H2O_l = water vapor concentration inside leaf. Gas exchange results with and *were significantly different from the control treatment.

high soil moisture treatment were not different between the control and optimal treatment, as the plants were well-watered and not under any stress. The optimal seed and water treatment had a total cumulative water savings of 49% ((20,950 – 10,650 ml)/20,950 ml) x 100 = 49) for the low soil moisture treatment.

Whole plant water use efficiency increased for the optimal seed and water treatment for the low soil moisture target. Whole plant WUE for the control treatment was 0.08 g/ml (32.9 g/403 ml/day) versus 0.15 g/ml (31.1 g/205 ml/day) for the optimal seed and water treatment for the low soil moisture target (WUE parameters were taken from Table **11**). This represents an 87% increase in whole plant WUE for the optimal seed and water treatment. Also, there was a 40% increase in whole plant WUE for the optimal treatment for the high soil moisture target. The whole plant WUE represents the oven-dry biomass produced per ml of water based on daily watering volumes averaged over the 60-day study period.

The optimal seed and water treatment effects on cooling efficiency (Tleaf/Tair) were also tested. The cooling efficiency was 0.996 and 0.983 for the control and optimal treatments for the low soil moisture target. These results show leaf temperatures were cooler than air temperatures, even when measured under high water stress. However, the optimal seed and water treatment didn't significantly increase the cooling efficiency compared to the control.

The third efficiency test involved the effects of the optimal treatment on carbon assimilation efficiency ((g biomass/day)/Pn (umol $CO_2/m^2/s$)). The average daily biomass growth rate was 0.522 (32.9 g/63 days) and 0.493 g/day (31.1 g/63 days) g/day for the control and optimal seed and water treatments (Parameters taken from Table **11**). The carbon assimilation efficiency was 0.050 (0.5222 g/day/10.41 umol $CO_2/m^2/s$) and 0.083 oven-dry g/day/umol $CO_2/m^2/s$ (0.493 g/day/5.92 umol $CO_2/m^2/s$) for the control and optimal treatments for the low soil moisture target (Parameters taken from Table **11**). In terms of total, oven-dry, aboveground biomass, the control treatment had 32.9 g versus 31.1 g for the optimal treatment. However, when the total biomass is converted to an average daily growth rate per umol $CO_2/m^2/s$ of carbon assimilated during photosynthesis, the carbon assimilation efficiency for the optimal seed and water treatment increased by 66% over the control. These results show that overall plant efficiency improves when the seeds are magnetized and seedlings are irrigated with SW water.

The water vapor gradient between the intercellular water content and atmospheric air can be quantified by water vapor pressure (vpdl) or molar water concentration (h2o_diff). Water vapor is transported down the pressure gradient between the leaf and air. Consequently, leaf transpiration rates should positively correlate with these water vapor gradient variables. However, vapor transport is regulated by the stomata to reduce excess water loss during water stress conditions. As the water vapor gradient increases, both vpdl and h2o_diff increase to reflect the increased strength of the gradient. Therefore, transpiration should decrease as the strength of the water vapor gradient increases to minimize excessive water vapor losses.

The unlinking of transpiration with water vapor dynamics was investigated using regression analysis. Linear regression tests were conducted for transpiration and vpdl and H2O-diff (Figure **2**). As expected, there was a negative, linear relationship between transpiration and vpdl and h2o-diff for the control treatment. Water stressed plants initiate defense activities such as stomata closure to limit excessive water losses due to the strong water vapor gradient between the leaf and air. Watering with SW water converted this relationship into a positive linear regression for the optimal seed and water treatment for both vpdl and h2o_diff (Figure **2**). In other words, as the water vapor gradient increased with increased risk for water vapor losses, transpiration also increased. This positive relationship unlinks the stomata function of regulating water loss in water stressed plants.

Linear regression tests were also conducted for transpiration, stomatal conductance, and leaf temperature for the low soil moisture target treatment (Figure **3**). These regression plots mirrored the transpiration plots in Figure **2**. There was a negative relationship between transpiration and conductance and leaf temperature for the control treatment. However, there was a positive relationship between these two variables and leaf temperature for the magnetized seed plus 2 MT + HWT treatment, which had the second-best gas exchange results. The optimal seed and water treatment had too few data points (3 data points) to run a valid regression test.

The two sets of regression plots clearly reveal the typical plant defense activity of partially closing the stomata and restricting transpiration for water-stressed plants for the control treatment. In contrast, the typical suite of regulatory plant defenses to high water stress was deactivated for the optimal seed and water

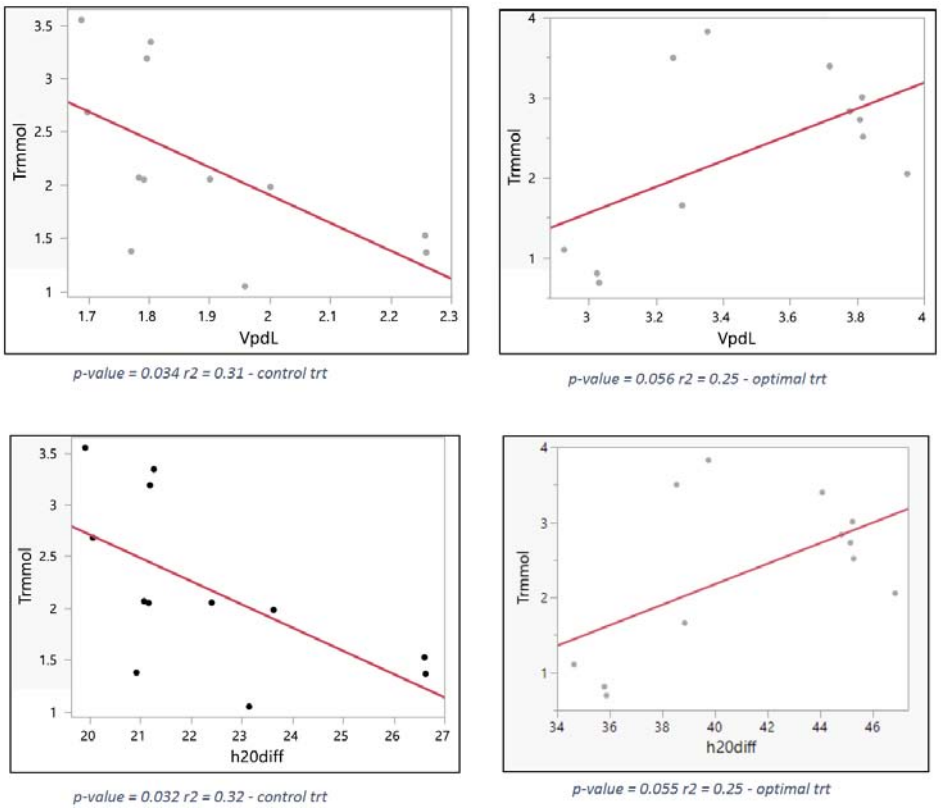

Figure 2: Linear regression of transpiration over vpdl and h2o_diff for control and optimal treatment. The regression included all three soil moisture levels. The Control treatment with no magnetized seeds. and 0 MT + NHWT are the left-side graphs, and the optimal treatment with the magnetized seeds and 10 MT + HWT water treatment are the right-side graphs.

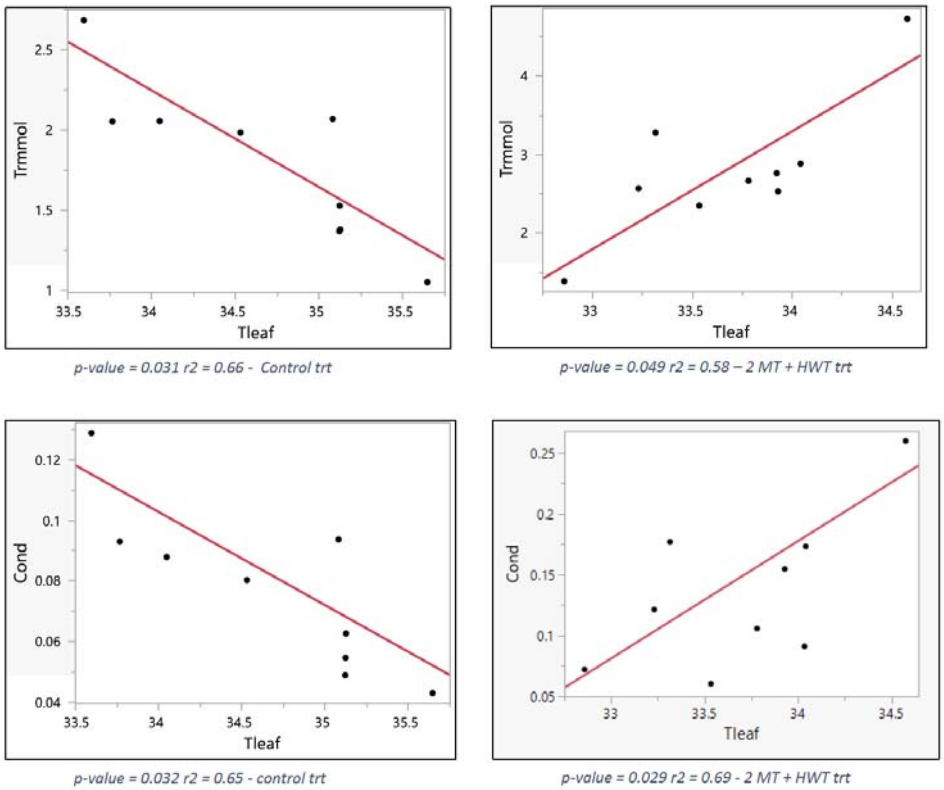

Figure 3: Linear regression of transpiration and stomatal conductance over leaf temperature for the control (left column) and magnetized seed plus 2 MT + HWT treatments (right column) for the low soil moisture treatment.

treatment. In both regression tests, transpiration rates increased with increasing strength of the water vapor gradient and leaf temperature for the optimal treatment. Also, stomatal conductance increased with increasing air temperature. The discussion section offers possible explanations of the underlying mechanisms for deactivating this suite of regulatory defense activities in the optimal treatment.

4. DISCUSSION

Daily watering was reduced 21 days after planting, and soil moisture levels were monitored until the three irrigation target levels were reached (Figure **1**). Leaf wilting symptoms were observed each morning. Short-term wilting appeared when volumetric soil moisture levels were below 10% (v/v). Wilted leaves generally returned to full turgor after watering each morning, indicating that the plants were under moderate water stress for the low and medium water irrigation targets. The soil volume in 3.8 l pots had limited water holding capacity, making maintaining even semi-stable soil moisture conditions challenging. At the end of the study, the velvet bean plants ranged in height from 3 to 4 m and had an estimated leaf area per plant that ranged from 3,000 to 5,000 cm^2 (Images **2-4**). Under the high soil moisture target, the large plants readily transpired up to 1,000 to 1,500 ml of water daily by the end of the study. As the plants grew to the top of the three-meter stakes, the daily water volume gradually increased to adjust for higher transpiration rates and to maintain the target soil moisture levels.

In the first article by Ramsey [1], analyses of the cumulative or the total water volume added per pot for each treatment revealed that the optimal seed and water treatment resulted in significant water savings. Depending on the three soil moisture levels, the water use savings ranged from 29% to 49 % for the optimal seed and water treatment. The optimal treatment had a water savings of 49 and a 41 % reduction in total water usage for the high and low soil moisture treatment. Also, the optimal seed and water treatment had a 6.8 % decrease in oven-dry foliage biomass compared to the control treatment for the low soil moisture target.

Transpiration rates were related to the differential in water vapor and water concentration between the leaf intercellular airspace and air (Figure **2**). As the differential increased for these two water parameters, there was a negative linear reduction in transpiration for the control treatment across all soil moisture target treatments. Water-stressed plants defend against high water vapor gradients or vpdl levels by partially closing stomata and reducing transpiration rates to minimize excessive water vapor losses [27]. Plants irrigated with SW water altered the water content dynamics in the intercellular airspaces due to increased BSW levels within the leaves. The two regression test sets (Figures **2**, **3**) agree with the correlation tables involving the vpdl and h20_l parameters (Tables **6-10**).

Macroscopic coherence allows plants to synchronize activities and systems across multiple biological scales to efficiently and rapidly adapt to ever-changing environmental conditions [33 – 35]. The overall results for multivariate tests imply that macroscopic coherence exists in the plants to deactivate the highly interconnected suite of plant defenses in a timely manner (Tables **6-10**). Eight gas exchange variables in the multivariate tables were related to regulatory plant defenses. Evidence for deactivation of the regulatory plant defenses for the optimal treatment was implied by the lack of pairwise correlations among the highly interconnected suite gas exchange variables. There were 24 significant correlations among all the pairwise comparisons in the control treatment, while there was only one significant correlation among the eight foliage variables for the optimal treatment. The lack of correlation among the interconnected variables implies that only macroscopic coherence could have efficiently and rapidly synchronized the deactivation of a large suite of interconnected regulatory defense activities without undue plant injury.

A follow-up multivariate test was conducted for the control and optimal seed and water treatments for the low soil moisture target treatment. This multivariate test included eight leaf and leaf water content variables, one soil variable, five atmospheric variables, and two ratio variables (WUE and Ci: Ca) for a total of 16 variables for leaf, water, soil, and air measurements. A total of 137 paired correlation tests were conducted among the 16 variables. The control treatment had 42 significant correlations, while the optional seed and water treatment had only nine significant correlations.

The 42 significant paired correlations in the control treatment are strong evidence of considerable interconnectivity among the 16 variables. These gas exchange variables directly involve the regulatory plant defense activities needed to minimize plant injury due to extreme water stress, i.e., soil moisture averaged 2% v/v for the control treatment. These regulatory

activities of the plant defense system come at a metabolic cost. If the number of significant correlations is assumed to be a quasi-quantitative surrogate for metabolic costs, then the number of significant correlations is directly related to metabolic costs. The percentage of significant correlations to the total paired correlations was 7 and 31% for the optimal and control treatments. This represents a 4 to 5-fold decrease in significant correlations for the optimal treatment. In other words, there was a 4 to 5-fold increase in metabolic efficiency for the optimal treatment, assuming that significant, interconnected correlations in plant defense activities are a reliable biomarker for metabolic defense costs.

The three plant efficiency tests show that the whole plant WUE increased by 87% for the optimal seed and water treatment under the low soil moisture target. Also, there was a 66% increase in carbon assimilation efficiency for the optimal seed and water treatment under the low soil moisture target. In addition, the optimal treatment saved 49% of the watering volume compared to the control treatment for the low soil moisture target. There was an 8.5-fold increase in soil moisture for the optimal treatment for the low soil moisture target. There was a 43% reduction in photosynthesis but a six-fold increase in stomatal conductance for the treatment, implying an increase in metabolic efficiency. Finally, there was a 68% reduction in the Ci/Ca ratio for the optimal treatment, indicating a significant reduction in internal CO_2 requirements for photosynthesis. These results show that the magnetized seed and SW water treatment significantly enhanced the overall plant and metabolic efficiency.

Macroscopic coherence resulted in the efficient synchronization of maintaining metabolic efficiency, deactivation of regulatory defense activities, and minimizing plant injuries for the optimal seed and water treatment in the low soil moisture target treatment. Macroscopic coherence has a higher, more integrated role in the synchronization of multi-scale plant systems to achieve metabolic and water use efficiency while increasing resilience for the optimal treatment.

Liquid water undergoes a phase transition from liquid to gas in the spongy mesophyll, an endothermic process to cool the foliage. This heat-absorbing process requires 2,256 J of energy to convert a gram of liquid water into water vapor [36]. Phase transition rates are regulated by water properties such as vapor pressure, latent heat of vaporization, and viscosity [37 - 38]. These water properties are a function of the extent of the hydrogen bond network, the number of supramolecular water clusters, and the strength of the hydrogen bonds in SW or BSW water. The phase transition rate decreases with lower vapor pressure and higher latent heat of vaporization and viscosity parameters. This study assumes that plants under high water stress have inadequate levels of BSW water and are at risk of excessive water vapor losses. The underlying hypothesis of irrigating plants with SW water is to maintain normal levels of BSW water for plants grown under high water stress and reduce the risk of excessive water vapor losses.

The unexpected results from the two regression test sets (Figures **2**, **3**) could be explained by the increased phase transition threshold due to higher BSW water levels in the SW-watered plants. The higher BSW water levels lowered the vapor pressure and increased the latent heat of evaporation of the liquid phase. The phase transition threshold for SW water shifts toward higher temperatures, which reduces transition rates from liquid to gas phase during minor increases in leaf temperatures. In other words, the water content remained in the liquid phase for the SW-watered plants under higher foliage temperatures in the low soil moisture treatment compared to the control treatment.

The higher the vapor pressure at a given temperature, the higher the phase transitions from liquid to gas. The vapor pressure of 100% SW water is 0.01 and 0.1255 kPa at -40 and -20 C, respectively [39 - 40]. In contrast, liquid water has a vapor pressure of 3.17 kPa at 25 C, a 99% increase in vapor pressure over 100% structured water. In other words, liquid water has a 99% higher vapor pressure than SW water. The control treatment had a lower phase transition threshold; thus, the risk of excessive water vapor losses was higher at lower foliage temperatures. To reduce the risk of foliage injury and photoinhibition due to excessive water vapor losses, a suite of regulatory defense activities was activated for the control treatment. The SW-watered plants maintained their liquid phase BSW water levels at a higher temperature threshold, thereby avoiding costly regulatory plant defense activities.

The latent heat of vaporization (J mol/mol H2O) also affects the phase transition of liquid water to water vapor. The heat of vaporization is the energy needed to transition liquid water into water vapor [41]. The latent heat of vaporization of liquid, unstructured water is approximately 45.05 kJ /mol H_2O at 100 C (10.77 kcal) [41]. A study by Cenkowski *et al*. [42] indirectly

estimated the latent heat of vaporization of BSW water by measuring the additional energy needed to remove bound water from foods and grains. They found that vegetable or grain moisture content ranged from 10% to 20%. Their results show that the heat of vaporization for bound, or BSW water, ranged from 47.25 to 56.25 kJ/mol H_2O when the moisture content ranged from 10 to 20% in vegetables or grains. In contrast, the heat of vaporization of free water was 45.05 kJ/mol H_2O [41]. In other words, the heat of vaporization of bound water was about 1.05 to 1.25 higher than for free, unstructured water. However, this thermodynamic water property was measured under laboratory conditions. Leaf temperatures only ranged from 30.7 to 39.1 C (303.15 to 312.15 K) in the gas exchange data. This temperature range is equivalent to an energy differential of 4.18×10^{-24} to 4.31×10^{-24} kJ of energy [43]. In other words, a 9 C increase in leaf temperatures only increases the energy levels by 0.13 x 10^{-24} kJ. The physiological constraints of leaf temperature dynamics may only cause minor increases in energy levels that relate to the latent heat of vaporization in leaf tissue water. The leaf temperature relationship with the latent heat of vaporization should be considered when estimating the phase transition thresholds for low and normal levels of BSW water in plant tissue.

A third water property related to the phase transition from liquid to water vapor is viscosity. Angel1 [44] estimated the shear viscosity of supercooled water to be approximately 150 MPa. Gao *et al*. [45] found that pure water confined to sub-nanometer gaps developed hexagonal lattice layers with a four-order magnitude increase in viscosity, i.e., a 10,000 x increase over pure water viscosity of 10^{-8} MPa. The increased viscosity of BSW interfacial water requires higher temperatures to reach the phase transition threshold before BSW water in the spongy mesophyll transits into water vapor.

The ability to maintain normal or adequate levels of BSW water in water-stressed plants significantly improves drought tolerance and resilience to abiotic stressors. In addition to the previously mentioned SW water properties, there is another water property that is very obscure but, if proven valid, has a critical role in plant water transport. Pollack formulated his 'proton drive theory"[46] based on his Exclusion Zone (EZ) theory as an alternative water transport theory in plants. The widely accepted water cohesion theory states that water is transported in xylem vessels under negative pressure created by leaf transpiration. His EZ water zone theory states the BSW (EZ) water zone excludes all solutes and ions, including hydronium ions, that are repelled into the free water zone adjacent to the interfacial water zone. The proton drive theory states that the electrostatic charge properties of BSW water 'push" or repel water through the plant vascular system. To support this theory, Pollack published a crypto image of a xylem vessel infused with ink microspheres taken with a transmission electron microscope (TEM) [46]. The TEM image clearly shows an EZ zone on both walls of the xylem, with the ink sphere excluded or repelled into the middle of the xylem vessel.

The hydronium ion drive theory states that energy inputs such as infrared energy from sunlight or respiration energize free water so that it can self-assemble into BSW water. As the BSW (EZ) zone increases, the hydronium ions (H_3O^+) concentration also increases, and the ions are expelled out of the EZ zone into the bulk, free water zone. The positive charges within the concentrated zone of expelled hydronium ions repel the H_3O^+ ions up the xylem vessels, creating sap flow against the pull of gravity [46]. Although xylem vessels are dead cells, the lignin component in the xylem walls has a negative charge of -30 mV [47]. This same principle also forces water to move autonomously in horizontal inanimate tubes that can form EZ water. In essence, the concentration of hydronium ions repel each other and are also attracted to the negative charges in lignin and cellulose, providing the driving forces needed to transport liquid water in plants. This theory is validated by numerous sap flow studies that show that sap exposed to infrared frequencies has increased flow rates [48 – 51]. The hydronium ion drive theory and numerous sap flow studies suggest that maintaining or increasing the BSW water levels in xylem vessels stabilizes sap flow rates for plants under water stress.

Plant research reveals that plants' BSW or bound water levels correlate with increased freeze or drought tolerance [52 – 61]. Zhang *et al*. [52] found that terahertz spectroscopy could remotely measure plant leaves' free and bound water content. Zhang *et al*. [53] also evaluated the ability of terahertz spectroscopy to quantify free and bound water in citrus leaves exposed to low temperature stress. They found that the relative change in volume fraction for the bound: free water ratio increased by 9-fold after five freeze-thaw cycles for citrus leaves. They also found that the relative change in volume fraction of bound water increased by

5-fold after five freeze-thaw cycles for citrus leaves. Singh *et al*. [54] also evaluated the ability of terahertz spectroscopy to measure leaf water content. These findings show that it is now possible to quantify the amount of bound water in plant tissue using non-invasive spectroscopy instruments.

Rascio *et al*. [55] investigated two wheat genotypes (*Triticum durum*) grown under water stress conditions. The first wheat genotype had a regular cell affinity for bound water or BSW water, and the second wheat genotype was a mutant genotype with a higher affinity for bound water. They found that the mutant wheat genotype with higher levels of bound, or BSW water, had significantly lower leaf temperature than the non-mutant genotype even as the air temperature increased to 35 C. They also found that the mutant genotype had about 66% lower transpiration rates than the non-mutant genotype. Another genotype study by Rascio *et al*. [56] found that the drought-tolerant wheat genotype had a higher level of bound water in the wheat foliage.

Drought tolerance studies involving cotton by Ergashovich *et al*. [57] and Singh *et al*. [58] show a correlation between bound water levels in the foliage and increased tolerance to water stress. Jecmenica *et al*. [59] found that bound water in common bean foliage increased root length when bean plants were grown at 30 C. Zhang *et al*. [60] found that the ratio of bound water to free water increased in water-stressed sugar cane that had a foliage chemical treatment. Wang *et al*. [61] studied the effects of hot, dry summers on a drought resistant C4 tussock grass (*Heteropogon contortus*) used for grazing in China. They found that the bound water to free water ratio (BW: FW ratio) was the most sensitive parameter for measuring water stress sensitivity. Also, they found that the BW: FW ratio was 152% higher in the drought-resistant tussock grass grown at 4 % soil moisture compared to the control treatment grown at 10%. An ecological study by Yukui *et al*. [62] found that the BW: FW ratio was correlated with drought resistance in desert shrubs. Other studies show more indirect findings involving correlations between bound water in plants and their ability to increase drought tolerance or resistance. It is evident from this literature that the ability of a plant genotype or species to increase its BSW water levels also increases its ability to minimize environmental abiotic stressors such as water, heat, or cold stress.

5. CONCLUSION

The vapor pressure, latent heat of vaporization, and hydronium ion (H_3O^+) exclusion properties of BSW water dovetail seamlessly together to regulate and maintain homeostasis in the interplay between plant and water dynamics. The level of BSW water in plant tissue and vascular system is directly related to plant or crop resilience to abiotic stressors. The multivariate test shows that many gas exchange parameters are highly interconnected and regulated by the plant defense system for the control treatment. The optimal seed and water treatment had a synchronistic effect on enhancing metabolic efficiency by increasing whole plant WUE by 87% and carbon assimilation efficiency by 66%. The optimal seed and water treatment deactivated a suite of regulatory plant defenses while simultaneously ensuring minimal plant injury for plants grown under high water stress for 35 to 40 days. Three BSW water properties, vapor pressure, latent heat of vaporization, and hydronium ion exclusion, were offered as possible underlying mechanisms for improving water dynamics in the optimal seed and water treatment. The three BSW water properties contributed to enhanced water transport, water vapor dynamics, and gas exchange responses in the optimal seed and water treatment. Maintaining optimum efficiency and minimal injury in a four-meter-tall legume seems highly improbable without macroscopic coherence synchronizing all the highly interconnected plant systems. Recent research shows strong evidence that plants have such quantum biology properties as quantum coherence, macroscopic coherence, tunneling, and entanglement [63 - 64]. This opens up promising new research avenues to enhance overall plant resilience and health for crops exposed to biotic and abiotic stressors.

REFERENCES

[1] Ramsey CL. Application of a structured water generator for crop irrigation: Structured water, drought tolerance, and alteration of plant defense mechanisms to abiotic stressors. J Basic Appl Sci 2021; 17: 127-52. https://doi.org/10.29169/1927-5129.2021.17.14

[2] Sidorenko G, Brilly M, Laptev B, Gorlenko N, Antoshkin L, Vidmar A, Kryžanowski A. The Role of Modification of the Structure of Water and Water-Containing Systems in Changing Their Biological, Therapeutic, and Other Properties Overview. Water 2021; 13(17): 2441. https://doi.org/10.3390/w13172441

[3] Stekhin AA, Yakovleva GV, Pronko KA, Zemskov AP. Quantum biophysics of water. Clinical Practice 2018; 15(3): 579-86. https://doi.org/10.4172/clinical-practice.1000393

[4] Zhang Z, Li D, Jiang W, Wang Z. The electron density delocalization of hydrogen bond systems. Advances in Physics: X 2018; 3(1): 1428915. https://doi.org/10.1080/23746149.2018.1428915

[5] Chaplin MF. Water's hydrogen bond strength. Water and Life: The unique properties of H2O 2010; 1. https://doi.org/10.1201/EBK1439803561-c5

[6] Neela YI, Mahadevi AS, Sastry GN. Hydrogen bonding in water clusters and their ionized counterparts. The Journal of Physical Chemistry B 2010; 114(51): 17162-71. https://doi.org/10.1021/jp108634z

[7] Pang XF. Water: molecular structure and properties. World Scientific; 2014. https://doi.org/10.1142/8669

[8] Chaplin M. 2007. https://www.researchgate.net/publication/1769361_Water's_Hydrogen_Bond_Strength/references.

[9] Jhon MS. The water puzzle and the hexagonal key Amerika, Uplifting 2004.

[10] Lindinger MI. Structured water: effects on animals. Journal of Animal Science 2021; 99(5): 063. https://doi.org/10.1093/jas/skab063

[11] Lo A and Lo S. A Soft Matter State of Water and the Structures it Forms, 2012 https://www.researchgate.net/publication/274815653_A_Soft_Matter_State_of_Water_and_the_Structures_it_Forms?enrichId=rgreq-a600d8378f3b7ab0e72b6236be7201a7-

[12] Chaplin M. website. https://water.lsbu.ac.uk/water/water_sitemap.html

[13] Yakhno T, Yakhno V. Virtual and Real Water. What is the Difference?

[14] Messori C, Prinzera SV, di Bardone FB. Deep into the water: exploring the hydro-electromagnetic and quantum-electrodynamic properties of interfacial water in living systems. Open Access Library Journal 2019; 6(05): 1. https://doi.org/10.4236/oalib.1105435

[15] Messori C, Prinzera SV, di Bardone FB. The super-coherent state of biological water. Open Access Library Journal 2019; 6(02): 1. https://doi.org/10.4236/oalib.1105236

[16] Davidson RM, Lauritzen A, Seneff S. Biological water dynamics and entropy: a biophysical origin of cancer and other diseases. Entropy 2013; 15(9): 3822-76. https://doi.org/10.3390/e15093822

[17] Ho MW. Water is the means, medium, and message of life. International J Design & Nature and Ecodynamics 2014; 9(1): 1-2. https://doi.org/10.2495/DNE-V9-N1-1-12

[18] Ho MW. Illuminating water and life. Entropy 2014 Sep; 16(9): 4874-91. https://doi.org/10.3390/e16094874

[19] Spartan Environmental Technologies. https://spartanwatertreatment.com/

[20] Clear Comfort at https://clearcomfort.com/controlled-environment-agriculture-water.

[21] Denkewicz, R. "The Power of Three." Water Quality Products (June 2015): 16-19.

[22] Ibrahim IH. Biophysical properties of magnetized distilled water. Egypt J. Sol 2006; 29(2): 363-9. https://doi.org/10.21608/ejs.2006.149287

[23] Jung YJ, Oh BS, Kang JW. Synergistic effect of sequential or combined use of ozone and UV radiation for the disinfection of Bacillus subtilis spores. Water Research 2008; 42(6-7): 1613-21. https://doi.org/10.1016/j.watres.2007.10.008

[24] Nobel PS. Physicochemical & environmental plant physiology. Academic Press; 1999.

[25] Rockwell FE, Holbrook NM, Jain P, Huber AE, Sen S, Stroock AD. Extreme undersaturation in the intercellular airspace of leaves: a failure of Gaastra or Ohm? Annals of Botany 2022; 130(3): 301-16. https://doi.org/10.1093/aob/mcac094

[26] Buckley TN, Sack L. The humidity inside leaves and why you should care: implications of unsaturation of leaf intercellular airspaces. American Journal of Botany 2019; 106(5): 618. https://doi.org/10.1002/ajb2.1282

[27] Grossiord C, Buckley TN, Cernusak LA, Novick KA, Poulter B, Siegwolf R, Sperry JS, McDowell NG, Plant Responses to Rising Vapor Pressure Deficit. New Phytologist 2020; 226: 1550–1566. https://doi.org/10.1111/nph.16485

[28] Whitewoods CD. Riddled with holes: Understanding air space formation in plant leaves. PLoS Biology 2021; 19(12): e3001475. https://doi.org/10.1371/journal.pbio.3001475

[29] Yong JW, Wong SC, Farquhar GD. Stomatal responses to changes in the vapor pressure difference between leaf and air. Plant, Cell & Environment 1997; 20(10): 1213-6. https://doi.org/10.1046/j.1365-3040.1997.d01-27.x

[30] Conaty WC, Mahan JR, Neilsen JE, Constable GA. Vapor pressure deficit aids the interpretation of cotton canopy temperature response to water deficit. Functional Plant Biology 2014; 41(5): 535-46. https://doi.org/10.1071/FP13223

[31] Yan W, Zhong Y, Shangguan Z. A meta-analysis of leaf gas exchange and water status responses to drought. Sci Rep 2016; 6: 20917. https://doi.org/10.1038/srep20917

[32] Baligar VC, Elson M, He ZL, Li Y, Paiva AD, Ahnert D, Almeida AA, Fageria NK. Ambient and elevated carbon dioxide on growth, physiological and nutrient uptake parameters of perennial leguminous cover crops under low light intensities. International Journal of Plant & Soil Science 2017; 1-6. https://doi.org/10.9734/IJPSS/2017/32790

[33] Madl P, Renati P. Quantum Electrodynamics Coherence and Hormesis: Foundations of Quantum Biology. International Journal of Molecular Sciences 2023; 24(18): 14003. https://doi.org/10.3390/ijms241814003

[34] Geesink HJ, Jerman I, Meijer DK. Water, the cradle of life via its coherent quantum frequencies. Water 2020; 11: 78-108.

[35] Oschman JL. Functional role of quantum coherence in interfacial water. Proc Nat Acad Sci USA 2000; 97(7): 3183. https://doi.org/10.1073/pnas.97.7.3183

[36] Latent heat of vaporization. https://courses.lumenlearning.com/suny-physics/chapter/14-3-phase-change-and-latent-heat/#: ~: text=Phase%20changes%20occur%20at%20fixed,is%20the%20latent%20heat%20coefficient.

[37] Murphy DM, Koop T. Review of the vapour pressures of ice and supercooled water for atmospheric applications. Quarterly Journal of the Royal Meteorological Society: A journal of the atmospheric sciences, applied meteorology and physical oceanography 2005; 131(608): 1539-65. https://doi.org/10.1256/qj.04.94

[38] Osborne NS. Measurements of Heat Capacity and Heat of Vaporization of Water in the Range 0˚C to 100˚C. J Res Nat Bur Stand 1939; 23: 197-260. https://doi.org/10.6028/jres.023.008

[39] https://www.engineeringtoolbox.com/water-supercooled-vapor-pressure-d_1910.html

[40] https://en.wikipedia.org/wiki/Vapour_pressure_of_water

[41] Water – Heat of Vaporization. LibreText. https://bio.libretexts.org/Bookshelves/Introductory_and_General_Biology/Book%3A_General_Biology_(Boundless)/02%3A_The_Chemical_Foundation_of_Life/2.13%3A_Water_-_Heat_of_Vaporization#: ~: text=Water%20has%20a%20heat%20of%20vaporization%20value%20of%2040.65%20kJ%2Fmol

[42] Cenkowski S, Jayas DS, Hao D. Latent heat of vaporization for selected foods and crops. Canadian Agricultural Engineering 1992; 34(3): 281-6.

[43] Kelvin conversion. https://www.translatorscafe.com/unit-converter/en-US/energy/70-67/kelvin-hertz/

[44] Angell CA. Supercooled water. Annual Review of Physical Chemistry 1983; 34(1): 593-630. https://doi.org/10.1146/annurev.pc.34.100183.003113

[45] Gao J, Szoszkiewicz R, Landman U, Riedo E. Structured and viscous water in subnanometer gaps. Physical Review B 2007; 75(11): 115415. https://doi.org/10.1103/PhysRevB.75.115415

[46] Pollack GH. The Fourth Phase of Water. Beyond Solid, Liquid, and Vapor. Ebner and Sons Publishers: Seattle, WA, USA 2013.

[47] Siddiqui L, Bag J, Mittal D, Leekha A, Mishra H, Mishra M, Verma AK, Mishra PK, Ekielski A, Iqbal Z, Talegaonkar S. Assessing the potential of lignin nanoparticles as drug carrier: Synthesis, cytotoxicity and genotoxicity studies. International journal of biological macromolecules 2020; 152: 786-802. https://doi.org/10.1016/j.ijbiomac.2020.02.311

[48] Boini A, Bresilla K, Perulli GD, Manfrini L, Grappadelli LC, Morandi B. Photoselective nets impact apple sap flow and fruit growth. Agricultural Water Management 2019; 226: 105738. https://doi.org/10.1016/j.agwat.2019.105738

[49] Nemera DB, Dovjik I, Florentin A, Shahak Y, Charuvi D, Cohen S, Sadka A. Sparse-shading red net improves water relations in Valencia orange trees. Agricultural Water Management 2023; 289: 108533. https://doi.org/10.1016/j.agwat.2023.108533

[50] Zeppel MJ, Murray BR, Barton C, Eamus D. Seasonal responses of xylem sap velocity to VPD and solar radiation during drought in a stand of native trees in temperate Australia. Functional Plant Biology 2004; 31(5): 461-70. https://doi.org/10.1071/FP03220

[51] Zhao CY, Si JH, Feng Q, Yu TF, Li PD. Comparative study of daytime and nighttime sap flow of Populus euphratica. Plant Growth Regulation 2017; 82: 353-62. https://doi.org/10.1007/s10725-017-0263-6

[52] Zang Z, Li Z, Lu X, Liang J, Wang J, Cui HL, Yan S. Terahertz spectroscopy for quantification of free water and bound water in leaf. Computers and Electronics in Agriculture 2021; 191: 106515. https://doi.org/10.1016/j.compag.2021.106515

[53] Zang Z, Li Z, Wang J, Lu X, Lyu Q, Tang M, Cui HL, Yan S. Terahertz spectroscopic monitoring and analysis of citrus leaf water status under low temperature stress. Plant Physiology and Biochemistry 2023; 194: 52-9. https://doi.org/10.1016/j.plaphy.2022.10.032

[54] Singh K, Bandyopadhyay A, Bertling K, Lim YL, Gillespie T, Indjin D, Li L, Linfield EH, Davies AG, Dean P, Rakić AD. Comparison of Physical and System Factors Impacting Hydration Sensing in Leaves Using Terahertz Time-Domain and Quantum Cascade Laser Feedback Interferometry Imaging. Sensors 2023; 23(5): 2721. https://doi.org/10.3390/s23052721

[55] Rascio A, Altamura G, Pecorella I, Goglia L, Sorrentino G. Physiological mechanisms preventing plant wilting under heat stress: a case study on wheat (Triticum durum Desf.) bound water-mutant. Environmental and Experimental Botany 2023; 105502. https://doi.org/10.1016/j.envexpbot.2023.105502

[56] Rascio A, Platani C, Di Fonzo N, Wittmer G. Bound water in durum wheat under drought stress. Plant Physiology 1992; 98(3): 908-12. https://doi.org/10.1104/pp.98.3.908

[57] Ergashovich KA, Toshtemirovna NU, Raximovna AK, Abdullaevna FF. The properties of cotton resistance and adaptability to drought stress. Journal of Pharmaceutical Negative Results 2022; 13(4): 958-61.

[58] Singh V, Pallaghy CK, Singh D. Phosphorus nutrition and cotton tolerance to water stress: II. Water relations, free and bound water, and leaf expansion rate. Field crops research 2006; 96(2-3): 199-206. https://doi.org/10.1016/j.fcr.2005.06.011

[59] Jecmenica M, Kravić N, Vasić M, Živanović T, Mandić V, Damnjanović J, Dragičević V. Genetic variability of free energy in a function of drought tolerance in common bean accessions. Genetika 2016; 48(3): 1003-15. https://doi.org/10.2298/GENSR1603003J

[60] Zhang SZ, Yang BP, Feng CL, Chen RK, Luo JP, Cai WW, Liu FH. Expression of the Grifola frondosa trehalose synthase gene and improvement of drought-tolerance in sugarcane (Saccharum officinarum L.). Journal of Integrative Plant Biology 2006; 48(4): 453-9. https://doi.org/10.1111/j.1744-7909.2006.00246.x

[61] Wang XM, Zhao L, Yan BG, Shi LT, Liu GC, He YX. Morphological and physiological responses of Heteropogon contortus to drought stress in a dry-hot valley. Botanical Studies 2016; 57: 1-2. https://doi.org/10.1186/s40529-016-0131-0

[62] Yukui J, Fengmin LU, Jingbo ZH, Junliang G, Zhiming X, Fang L. Drought Resistance of Twelve Desert Shrubs at Seedling Stage of Ulan Buh Desert Ecosystem. Journal of Landscape Research 2016; 8(6): 83.

[63] Gagliano M, Renton M, Depczynski M, Mancuso S. Experience teaches plants to learn faster and forget slower in environments where it matters. Oecologia 2014; 175: 63-72. https://doi.org/10.1007/s00442-013-2873-7

[64] Kim Y, Bertagna F, D'souza EM, Heyes DJ, Johannissen LO, Nery ET, Pantelias A, Sanchez-Pedreño Jimenez A, Slocombe L, Spencer MG, Al-Khalili J. Quantum biology: An update and perspective. Quantum Reports 2021; 3(1): 80-126. https://doi.org/10.3390/quantum3010006